

# Missense VKOR mutants exhibit severe warfarin resistance but lack VKCFD via shifting to an aberrantly reduced state

Shuang Li,<sup>1</sup> Jie Sun,<sup>2</sup> Shixuan Liu,<sup>1</sup> Fengbo Zhou,<sup>1</sup> Michael L. Gross,<sup>2</sup> and Weikai Li<sup>1</sup>

<sup>1</sup>Department of Biochemistry and Molecular Biophysics, Washington University School of Medicine, St. Louis, MO; and <sup>2</sup>Department of Chemistry, Washington University in St. Louis, St. Louis, MO

## Key Points

- Severe warfarin resistant mutations change vitamin K epoxide reductase to aberrantly reduced states with uninhibited activity.
- High activity of reduced state compensates for mutants' defects, explaining general lack of vitamin K clotting factor deficiency.

Missense vitamin K epoxide reductase (VKOR) mutations in patients cause resistance to warfarin treatment but not abnormal bleeding due to defective VKOR activity. The underlying mechanism of these phenotypes remains unknown. Here we show that the redox state of these mutants is essential to their activity and warfarin resistance. Using a mass spectrometry-based footprinting method, we found that severe warfarin-resistant mutations change the VKOR active site to an aberrantly reduced state in cells. Molecular dynamics simulation based on our recent crystal structures of VKOR reveals that these mutations induce an artificial opening of the protein conformation that increases access of small molecules, enabling them to reduce the active site and generating constitutive activity uninhibited by warfarin. Increased activity also compensates for the weakened substrate binding caused by these mutations, thereby maintaining normal VKOR function. The uninhibited nature of severe resistance mutations suggests that patients showing signs of such mutations should be treated by alternative anticoagulation strategies.

## Introduction

Warfarin is an oral anticoagulant widely used to treat and prevent thromboembolic disorders including atrial fibrillation, deep venous thrombosis, and pulmonary embolism.<sup>1-8</sup> Warfarin hinders blood coagulation by lowering the levels of active vitamin-K-dependent clotting factors. The activity of these factors requires membrane association via a designated domain that contains multiple  $\gamma$ -carboxylated glutamate residues. The  $\gamma$ -carboxylation reaction is driven by the oxidation of vitamin K hydroquinone, which is converted to vitamin K epoxide (KO) after the reaction. To regenerate K hydroquinone, vitamin K epoxide reductase (VKOR) reduces KO first to the vitamin K quinone (K) and then to the hydroquinone; each reduction step is coupled to the oxidation of 2 cysteines at the VKOR active site.<sup>9</sup> This redox cycle of vitamin K occurs in the endoplasmic reticulum (ER), and warfarin blocks this cycle via specifically inhibiting the VKOR activity.<sup>10,11</sup>

Dose control of warfarin therapy is notoriously difficult. Underdosing may lead to thromboembolic events and overdosing can result in severe bleeding, which is sometimes fatal.<sup>12,13</sup> These difficulties arise from warfarin's narrow therapeutic index and wide interpatient variation. As the target of warfarin, VKOR is a key pharmacogenetic factor accounting for interpatient variation.<sup>14,15</sup> The US Food and

Submitted 16 June 2022; accepted 8 November 2022; prepublished online on *Blood Advances* First Edition 12 December 2022; final version published online 23 May 2023. <https://doi.org/10.1182/bloodadvances.2021006876>.

Data are available on request from the corresponding author, Weikai Li ([weikai@wustl.edu](mailto:weikai@wustl.edu)).

The full-text version of this article contains a data supplement.

© 2023 by The American Society of Hematology. Licensed under [Creative Commons Attribution-NonCommercial-NoDerivatives 4.0 International \(CC BY-NC-ND 4.0\)](https://creativecommons.org/licenses/by-nc-nd/4.0/), permitting only noncommercial, nonderivative use with attribution. All other rights reserved.

Drug Administration has included *VKOR* genotyping in the warfarin product label for dosage prediction. However, the clinical benefits of current predicting algorithms remain controversial.<sup>16</sup> In addition, current dosing algorithms do not consider a small subset of individuals who have an abnormally high dosage requirement<sup>17,18</sup> known as warfarin resistance (WR).

The WR phenotype is primarily caused by missense mutations in the coding region of *VKOR*.<sup>17,19-21</sup> The WR mutations are relatively rare and most are known from isolated case reports.<sup>15,19,20,22-24</sup> In a more comprehensive study, among 289 patients referred for investigation of abnormal warfarin dose (>20 mg/d), 8 of them (2.7%) carried WR mutations.<sup>18</sup> The NCBI database ([www.ncbi.nlm.nih.gov/SNP/snp\\_ref.cgi?locusid=79001](http://www.ncbi.nlm.nih.gov/SNP/snp_ref.cgi?locusid=79001)) reports the allele frequencies of only a few WR mutations, including L27V (0.003%), A34P/T/S (0.018% in Japanese populations), and V66M (0.009%).

For most patients carrying the WR mutations, an International Normalized Ratio (INR) in the therapeutic range (2-3) can be stably reached after trial-and-error dosing. In severe cases, however, the INR cannot be controlled even with very high warfarin doses. Consequently, the anticoagulation therapy must be aborted. These mutations are defined as “complete” resistance, in contrast to the “partial” resistance mutations for which stable INR is achievable.<sup>17,25</sup> Understanding the cause of resistance severity may improve the ability to predict warfarin dosage and the choice for alternative anticoagulation treatment.

Intriguingly, patients and their family members carrying the WR mutations do not exhibit abnormal bleeding due to vitamin K clotting factor deficiency (VKCFD). VKCFD is a spontaneous bleeding symptom caused by defects in the vitamin K cycle.<sup>26,27</sup> Although many mutations have been identified in the  $\gamma$ -carboxylase,<sup>28,29</sup> only 1 *VKOR* mutation, p.Arg98Trp, is associated with the VKCFD phenotype.<sup>27</sup> This mutation causes mislocalization and degradation of the *VKOR* protein and reduces most of its activity, but the mutation is not associated with WR.<sup>27</sup> On the other hand, most WR mutations are located near the *VKOR* active site (Figure 1A-B) where they may hinder substrate binding and/or catalysis. The defective *VKOR* proteins, however, only exhibit WR and do not cause VKCFD. In other words, although warfarin and substrates bind to the same active site pocket, the WR mutations appear to only affect warfarin inhibition but not *VKOR* activity. Based on these data, the phenotypes of WR and VKCFD appear to have no correlation.

Here we show that severe WR mutations shift *VKOR* to an aberrantly reduced form. The reduced *VKOR* binds warfarin poorly but is highly reactive to substrates, generating a large warfarin-uninhibited activity that manifests as apparent WR. On the other hand, the increased activity compensates for defective substrate binding caused by the WR mutations. Consequently, these mutants exhibit severe WR but maintain near-normal *VKOR* activity and lack VKCFD. Identifying the cause of these phenotypes improves our ability to predict warfarin dosage.<sup>30</sup> The warfarin untreatable nature of severe WR suggests invoking alternative anticoagulation treatment.

## Methods

### Cloning and transfection

WR mutants of human *VKOR* were generated by Quikchange site-directed mutagenesis, using wild-type *VKOR* complementary DNA

in pBudCE4.1 vector as the template. The constructs were transfected into a HEK293 cell line with *VKORC1/VKORC1L1* knocked out and with a chimeric FIXgla-Protein C reporter.<sup>31-33</sup>

### Preparation of microsomes

Transfected cells were centrifuged at 400g and resuspended in 50 mM phosphate buffer, pH 7.4, containing 150 mM KCl and protease inhibitor cocktail. The cells were disrupted by passing through an 18G needle and centrifuged at 1300g at 4°C for 10 minutes. Microsomes were collected by ultracentrifugation at 138 000g for 30 minutes and resuspended in 50 mM *N*-2-hydroxyethylpiperazine-*N'*-2-ethanesulfonic acid, pH 7.4, containing 20% glycerol. The concentration of total microsomal proteins was determined and adjusted using a bicinchoninic acid assay. The protein levels of *VKOR* mutants were analyzed by western blot (supplemental Figure 1) using the anti-*VKOR* antibody (Thermo Fisher Scientific).

### Microsomal activity assay

Catalysis of microsomal *VKORC1* was initiated in 500  $\mu$ L of buffer containing 40 mM reduced glutathione (GSH) or 5 mM dithiothreitol (DTT), 5  $\mu$ M KO, 150 mM KCl, and 200 mM *N*-2-hydroxyethylpiperazine-*N'*-2-ethanesulfonic acid, pH 7.5. The reaction was carried out at 30°C for 2 hours at different concentrations of warfarin and subsequently analyzed by high-performance liquid chromatography.<sup>33</sup>

### Cellular assay of warfarin's half maximal inhibitory concentration

The cellular carboxylation assay was performed as previously described.<sup>13,18</sup> The carboxylation level of secreted FIXgla-PC was measured by sandwich enzyme-linked immunosorbent assay using the cell-culture medium, with luciferase activity serving as the control for transfection efficiency. For half maximal inhibitory concentration (IC<sub>50</sub>) measurement, warfarin concentration range was optimized according to the warfarin response of different WR mutants.

### Live-cell MS-based quantification of *VKORC1* redox state

Mass spectrometry (MS) footprinting and quantification followed a protocol that we recently developed.<sup>32,34</sup> The fractions of reduced cysteines were calculated using the extracted ion chromatogram peak areas, NEM/(NEM + NEM-*d*<sub>5</sub>), of peptides bearing the *N*-ethylmaleimide (NEM) modification. The fractions of fully reduced (R), partially oxidized (PO), and fully oxidized (O) Cys132/Cys135 pair were calculated using the peak areas of 2NEM, NEM/NEM-*d*<sub>5</sub>, and 2NEM-*d*<sub>5</sub>, respectively, divided by those of 2NEM + NEM/NEM-*d*<sub>5</sub> + 2NEM-*d*<sub>5</sub>. For each cysteine or cysteine pair, 3 different peptides containing the cysteine(s) are used for the calculation.

### Molecular dynamics simulation

Crystal structure of human *VKOR* (PDB 6WVH) was used as the starting model with a brodifacoum ligand removed. The WR mutations were generated and models inserted into a 1-palmitoyl-2-oleoyl-glycero-3-phosphocholine (POPC) bilayer using CHARMM-GUI.<sup>35</sup> Molecular dynamics (MD) (100 ns) was performed with GROMACS MD simulation package<sup>36</sup> using CHARMM36m force field<sup>37</sup> and repeated 3 times. The root-mean-square fluctuation (RMSF) analysis was performed using GROMACS.

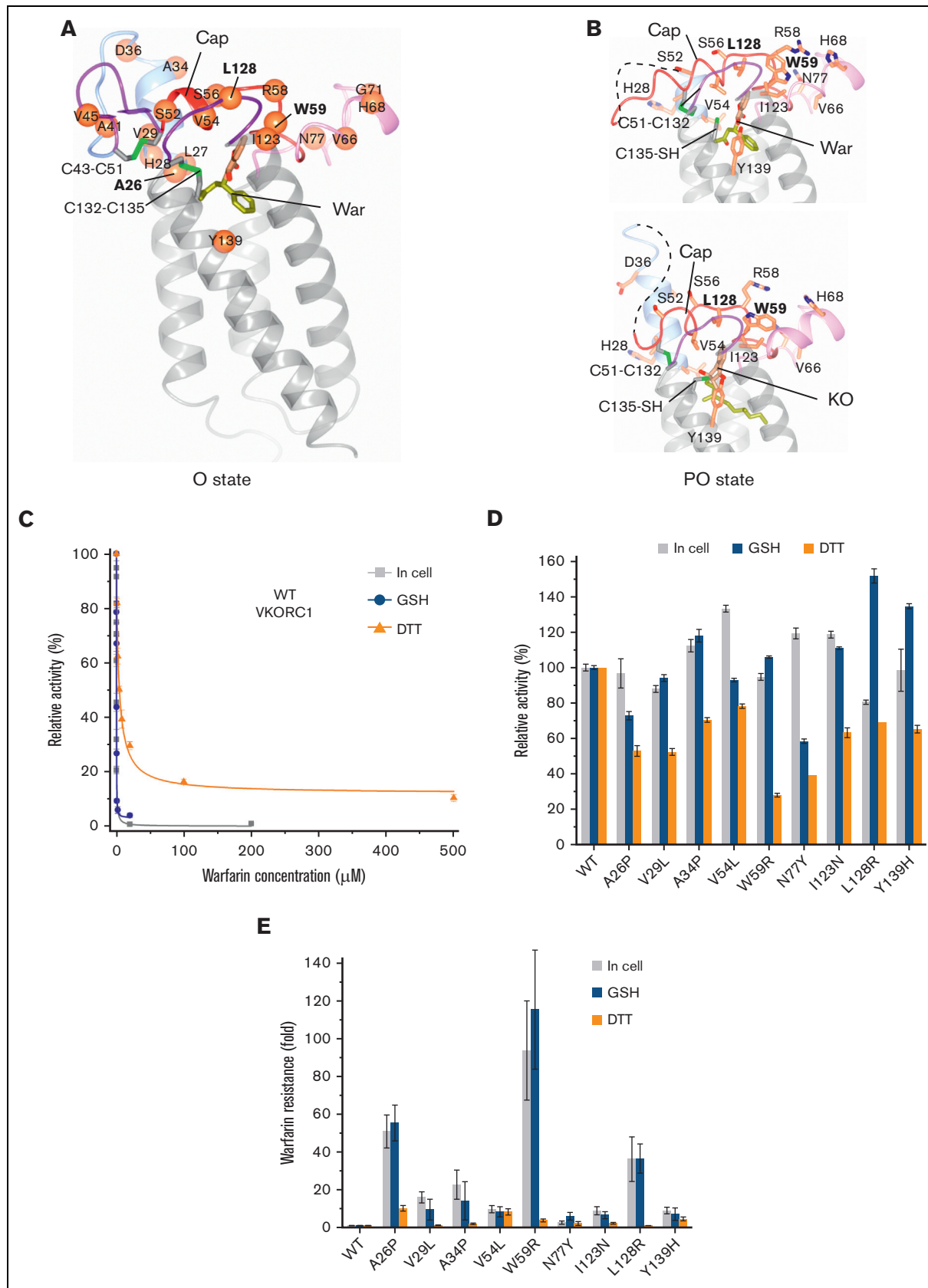


Figure 1.

## Results

### The VKCFD-lacking and WR phenotypes of missense VKOR mutants are associated with their redox state

To date, 27 naturally occurring WR mutations, located on 16 VKOR residues (Figure 1A), have been identified in 209 cases that require high warfarin dose<sup>38</sup> (Table 1). Investigating the causes of the WR phenotype, however, has been difficult, in part because most of these mutants do not show WR in traditional *in vitro* assays that use DTT to drive VKOR catalysis<sup>17</sup> (Table 1). For instance, a classic study from Lattard group shows that only 1 mutant, Ala26Pro, exhibits greater than fivefold WR<sup>40</sup> with the DTT-based assay (Table 1). Further, 10 out of the 25 expressed mutants show low or undetectable activity, to an extent that prohibited their IC50 measurement.

To overcome these difficulties, we built on a recent discovery that, for *in vitro* characterization, VKOR needs to be maintained in a redox state similar to that in the cells.<sup>33,41</sup> Because VKOR resides in the ER, which provides a relatively oxidized environment, most VKOR (~92%) is either in the PO or O state and only a small fraction (~8%) is in the R state.<sup>32,42</sup> The PO and O forms correspond to the formation of alternative disulfide bonds that determine the native, stable protein conformations of VKOR<sup>43</sup> (Figure 1A-B). In the O state, a Cys43-Cys51 disulfide bond stabilizes conformation of the extramembrane domain and a Cys132-Cys135 disulfide bond is formed within the transmembrane domain (Figure 1A). In the PO state, a Cys51-Cys132 disulfide bond links the VKOR extramembrane domain to its transmembrane domain and stabilizes the overall protein conformation (Figure 1B). These states can be maintained *in vitro* by using GSH,<sup>33,41</sup> a native reductant highly abundant in the ER.<sup>44,45</sup> Compared to DTT, GSH has a much higher redox potential that shifts VKOR to the relatively oxidized states present in cells<sup>32,42</sup> and maintains the stable conformations observed in crystal structures<sup>43</sup> (Figure 1A-B). Using GSH to drive the VKOR catalysis, we found that the inhibition curve of warfarin is nearly identical to that from the cell-based assay (Figure 1C). The IC50s are in the nanomolar range, corresponding to the estimated therapeutic concentration of warfarin.<sup>13-17</sup> In contrast, wild-type VKOR is weakly inhibited by warfarin in the presence of DTT (Figure 1C). The IC50 is in the micromolar range, similar to that reported previously.<sup>20,25</sup> This large discrepancy is because DTT reduces VKOR almost completely, generating an artificially R state that prohibits warfarin binding.<sup>32,33</sup> In cells, however, most wild-type VKOR is in the PO and O states that are preferentially inhibited by warfarin.<sup>46,47</sup> Maintaining wild-type VKOR in these relatively oxidized states (using GSH) preserves its warfarin sensitivity *in vitro*.

With this insight, we asked whether the phenotypes of WR mutants are also associated with their redox state. For this analysis, we selected all the WR mutants (9 in total) that showed

considerable resistance (> 5-fold) in the cell-based assay (Table 1). We first analyzed the activities of these WR mutants because defective VKOR may lead to VKCFD or abnormal bleeding. With their redox state maintained by GSH, all 9 WR mutants show a range from slightly lower to even higher activity (73%-152%) than the wild-type VKOR (Figure 1D), despite the relatively low expression level of certain mutants (eg, Leu128Arg; supplemental Figure 1). Consistently, in the cell-based assay, these mutants show 80% to 133% of the wild-type activity (Figure 1D), similar to previous reports.<sup>32,39,40</sup> Their high activity explains the general lack of VKCFD phenotype in patients and family members carrying the WR mutations (either homozygous or heterozygous). Their coagulation assay results are normal, and their serum KO level, a direct measure of defective VKOR activity or under-carboxylated prothrombin (PIVKA-II), are undetectable.<sup>18</sup>

In contrast, activities of all these WR mutants in DTT are lower (28%-78%) than the wild type, with Trp59Arg being the lowest (Figure 1D). These low activities suggest that the non-native state generated by DTT reduction together with the defect caused by the mutations hinder the catalysis of WR mutants. In contrast, GSH better preserves the activity of these mutants owing to the maintenance of their near-native redox and conformational state. The DTT-promoted activities in our microsomal assay, however, are higher than previously reported in detergents (Table 1), probably because the microsomes preserve the VKOR activity in the membrane environment and also enrich the VKOR protein, which is highly unstable in detergents.<sup>9,41</sup> Thus, the WR of all 9 mutants can be measured with DTT in subsequent analyses.

All 9 WR mutants in GSH exhibit resistance levels reflecting their reported clinical doses or resistance severities (Table 1). Further, the resistance levels correlate well with those known from cell-based assays (Figure 1E). The most resistant mutants are Ala26Pro (52-fold in GSH and 60-fold in cells), Trp59Arg (109-fold in GSH and 85-fold in cells), and Leu128Arg (33-fold in GSH and 40-fold in cells). Consistently, patients carrying these 3 mutations or other mutations on the same residues generally require very high doses and often fail to reach a stable INR of 2.0 to 3.0 (Table 1). Consequently, their warfarin therapy is frequently aborted.<sup>17,25,38,40</sup> The remaining 6 WR mutants show moderate resistance, 3- to 14-fold in GSH and 9- to 27-fold in cells. Similarly, the resistance phenotype of these mutations is relatively mild, and stable INR generally can be reached. In contrast, the apparent resistance levels with DTT are uncorrelated with clinical or cellular observations. Only Ala26Pro (10-fold) and Val54Leu (8-fold) show moderate resistance, and the other 7 mutants show little or no resistance (Figure 1E), consistent with previous reports.<sup>17,25</sup> Taken together, the differences between DTT and GSH show that maintaining the native redox state of WR mutants is the key to their activity and to WR.

**Figure 1. Redox state determines the warfarin sensitivity of wild-type VKOR and the resistance level and catalytic activity of WR mutants.** (A) Structural locations of the WR mutations (spheres) identified from patients. The mutations are either at the warfarin (War) binding pocket or at peripheral regions, stabilizing this pocket. The VKOR structure in the O state (PDB 6WV3) is shown. (B) VKOR structures in the PO state with warfarin (PDB 6WV4; top) and KO (PDB 6WV5; bottom). WR mutations (side chains) interfering with warfarin binding should also affect KO binding. The Cys51-Cys132 disulfide bond stabilizes the cap region despite the disorder of a preceding region (dashed line). (C) The warfarin inhibition curves of wild-type (WT) VKOR in cells and with GSH and DTT. Because DTT has a much lower redox potential than GSH, the overly reduced VKOR is not in the stable O or PO state (panels A-B) and is prohibited from binding warfarin. (D) Relative activities of WR mutants (normalized to WT). Activities of WR mutants in GSH are close to those observed in cells. In contrast, DTT reduction interferes with substrate binding that is further weakened by WR mutations, resulting in lower relative activities. (E) Resistance levels of WR mutants in GSH correspond well with their cellular resistance levels. With DTT, however, most WR mutants do not show resistance.

**Table 1. VKORC1 mutants at the proper redox state exhibit WR, reflecting their increased clinical doses, and patients carrying certain mutations are potentially untreatable by warfarin**

	WR (IC50 mutant/WT ± SEM)							Cases #	Typical dose (mg/d) <sup>25,38</sup>	Stable INR (2-3)	Uninhibited activity
	GSH	DTT		Cell							
	This study	This study	Lattard <sup>25</sup>	This study	Li <sup>32</sup>	Tie <sup>39</sup>	Oldenburg <sup>40</sup>				
WT	1.0 ± 0.2	1.0 ± 0.2	1.0 ± 0.7	1.0 ± 0.2	1.0 ± 0.2	1.0 ± 0.1	1.0 ± 0.2		4*	Yes	
<b>A26P*</b>	55.3 ± 9.5	10.1 ± 1.5	11.2 ± 6.4	50.8 ± 8.8	60.4 ± 13.2	72.0 ± 9.4	49.6 ± 7.2	1	20	<b>No</b>	<b>41%</b>
A26T			1.3 ± 0.7			1.9 ± 0.4	3.0 ± 0.5	1	6	<b>No</b>	
L27V			1.1 ± 0.7		1.6 ± 0.3	1.4 ± 0.2	2.5 ± 0.5	1	7	Yes	
H28W			0.4 ± 0.3		2.5 ± 0.6	1.3 ± 0.2	2.9 ± 0.5	1	10 P†	Yes	
V29L	9.4 ± 5.6	1.1 ± 0.2	Low exp.	15.9 ± 2.9	20.7 ± 3.3	19.2 ± 4.2	5.5 ± 0.8	3	14	Yes	
A34P	14.1 ± 10.1	1.9 ± 0.4		22.6 ± 7.7	27.2 ± 2.6	19.4 ± 4.4		1	27	Yes	
D36G			0.4 ± 0.3		2.5 ± 0.4	2.1 ± 0.5	3.2 ± 0.5	1	20	Yes	
D36Y			1.1 ± 0.7			1.3 ± 0.2	3.8 ± 1.0	164	8-20	Yes	
A41S			1.1 ± 0.5		1.3 ± 0.3	1.9 ± 0.3		1	16	Yes	
V45A			0.7 ± 0.3		2.2 ± 0.5	2.6 ± 0.6	6.2 ± 0.9	1	45	No	
S52L			Low act.			23.3 ± 4.5	7.4 ± 1.1	1	9 P	No	
S52W			Low act.		4.5 ± 0.9	6.6 ± 1.2	5.7 ± 1.2	1	10 P	Yes	
V54L	8.2 ± 2.7	8.2 ± 1.6	4.8 ± 2.4	9.7 ± 2.0	11.8 ± 2.2	8.5 ± 1.6	4.5 ± 0.7	3	5-37	Yes	
S56F			0.6 ± 0.6		2.2 ± 0.5	1.6 ± 0.3	6.8 ± 1.1	1	15 P	No	
R58G			0.9 ± 0.5		3.5 ± 0.8	6.0 ± 0.8	3.4 ± 0.6	4	34	Yes	
<b>W59R*</b>	115.4 ± 31.5	3.7 ± 0.7	Low act.	93.8 ± 26.3	84.9 ± 14.3	98.0 ± 12.8	17.5 ± 2.6	3	9 P	<b>No</b>	<b>27%</b>
W59C			0.7 ± 0.4			19.6 ± 3.0	7.6 ± 1.2	1	11 P	<b>No</b>	
<b>W59L*</b>			Low act.			84.5 ± 14.1	75.2 ± 11.0	1	15 P	<b>No</b>	
V66G			Low act.			3.9 ± 0.7	2.8 ± 0.5	1	8 P	Yes	
V66M			Low act.		3.3 ± 0.6	1.3 ± 0.2	5.4 ± 0.8	15	30	Yes	
H68T			3.8 ± 1.9			1.0 ± 0.2	5.1 ± 0.8	1			
G71A			Low act.			1.6 ± 0.2		1	6 P	No	
N77S			Low act.			6.0 ± 1.2	5.3 ± 1.0	1	9 P	No	
N77Y	5.9 ± 2.0	2.1 ± 1.0	Low act.	2.5 ± 0.9	9.4 ± 1.3	3.9 ± 0.6	3.9 ± 0.6	1	25	Yes	
I123N	6.5 ± 1.9	2.2 ± 0.4	2.4 ± 1.3	8.8 ± 2.2	9.0 ± 1.0	3.4 ± 0.5	8.5 ± 1.2	1	21 P	No	
<b>L128R</b>	36.5 ± 7.7	1.1 ± 0.2	Low act.	36.2 ± 11.8	39.7 ± 8.3	84.5 ± 14.6	49.6 ± 7.2	9	39-49	<b>No</b>	<b>22%</b>
Y139H	7.1 ± 3.3	4.4 ± 1.0	3.6 ± 2.0	8.9 ± 1.7	6.6 ± 1.0	4.7 ± 0.6	4.6 ± 0.7	1	9 P	No	

SEM, standard error of the mean; WT, wild-type.

\*Patients carrying these mutations (bold letters) are potentially untreatable by warfarin.

†P: Phenprocoumon is used.

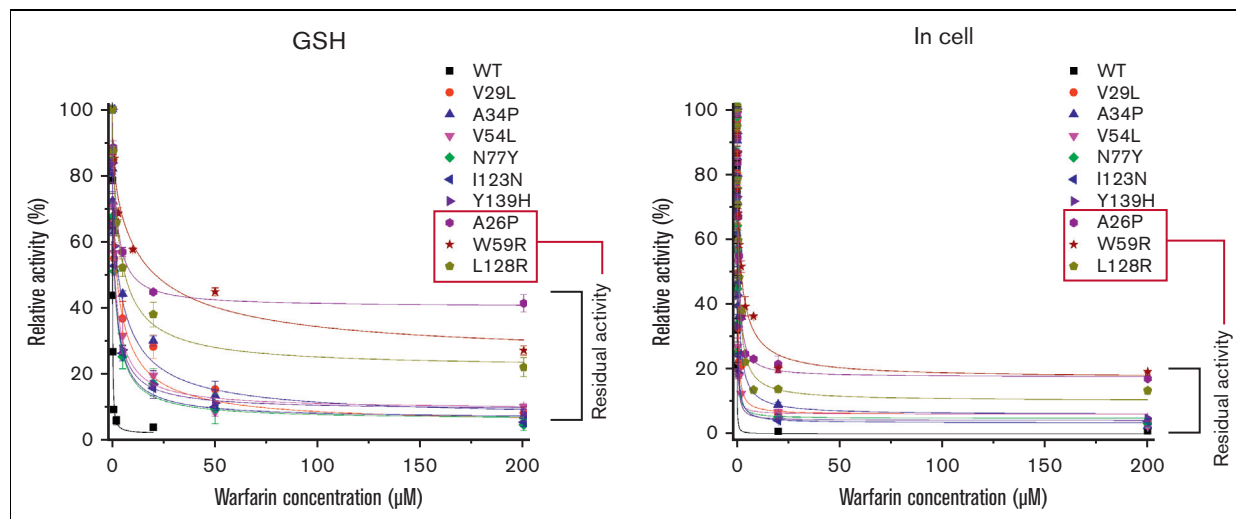


**Figure 2. Severe WR mutants show large residual activity that is uninhibited by warfarin.** Inhibition curves of strong WR mutants (> 5-fold resistance) in GSH (left) are similar to those in the cell-based assay (right), indicating that redox state is essential. The largest warfarin-uninhibited activity is observed for Ala26Pro, Trp59Arg, and Leu128Arg; patients carrying these mutations exhibit severe WR, and warfarin therapy is often aborted (Table 1). All error bars are from 3 replicates.

### Severe WR mutants retain high warfarin-uninhibited residual activity in vitro

The inhibition curves of strong WR mutants in GSH show a high level of residual VKOR activity (Figure 2) at warfarin concentrations (20–200  $\mu\text{M}$ ) that are several orders of magnitude higher than the therapeutic level – warfarin is in the nanomolar concentration when measured in blood.<sup>48</sup> The mutants showing the largest effects are Ala26Pro, Trp59Arg, and Leu128Arg, which retain 41%, 27%, and 22% of activity, respectively, at 200  $\mu\text{M}$  warfarin. Similar residual activities of these 3 mutants are also observed in the cell-based system at 200  $\mu\text{M}$  warfarin concentration (Figure 2), consistent with previous reports.<sup>39,40</sup> This warfarin-uninhibited activity in cells can be reproduced in the GSH-based in vitro assay, reinforcing the key role of the VKOR redox state. Notably, the 3 mutants showing the strongest resistance (Figure 1E) also retain the largest residual activities at high warfarin concentrations (Figure 2). With a high level of activity uninhibited by warfarin, active clotting factors remain at a level permitting coagulation. Consequently, patients carrying these severe WR mutations are unable to reach targeted INR with warfarin treatment. Thus, severe WR phenotype is mostly caused by this warfarin-uninhibited residual activity.

### Uninhibited activity of severe WR mutants is due to their aberrantly reduced state

To understand the cause of the warfarin-uninhibited activity (Figure 2), we analyzed the redox state of WR mutants in cells, given the knowledge that redox state is associated with resistance. We compared the redox state of the 3 severe WR mutants, Trp59Arg, Ala26Pro, and Leu128Arg, with wild-type VKOR. Their redox state was assessed by MS-based footprinting that measures the reduced and oxidized fraction of each cysteine in these proteins. In this experiment (Figure 3A), reduced cysteines were labeled by NEM- $d_0$  in cells. After cell lysis, disulfide-bonded cysteines were further reduced and labeled by the deuterated isotopologue, NEM- $d_5$ , and the protein was digested to peptides. The relative modification

levels of  $d_0$  and  $d_5$  were measured in the appropriate peptides by quantitative liquid chromatography/MS at high mass resolving power and the ratio of the  $d_0$  and  $d_5$  isotopic modifications gave the redox state of each cysteine in the cells. The footprinting detected all 7 cysteines in VKOR (Figure 3B; supplemental Figure 2): Cys16, Cys85, and Cys96 are noncatalytic cysteines; Cys43 and Cys51 mediate the electron transfer or disulfide exchange with the active site; and Cys132 and Cys135 are at the active site.<sup>32</sup>

For wild-type VKOR, we found that the reduced fractions of Cys51 (5%) and Cys132 (14%) are small, whereas those of Cys43 (46%) and Cys135 (58%) are much larger (Figure 3C). In other words, Cys51 and Cys132 are primarily oxidized. Their high oxidation level is because they are nearly always involved in forming disulfide bonds, either 1 Cys51-Cys132 disulfide bond in the PO state, or 2 disulfide bonds, Cys43-Cys51 and Cys132-Cys135, in the O state. Our recent crystal structures show that either of these disulfide bond configurations can stabilize human VKOR in a closed conformation (Figure 1A-B).<sup>43</sup> In the severe WR mutants, however, the reduced fraction of Cys51 is drastically increased, to 19% in Ala26Pro, 16% in Trp59Arg, and 15% in Leu128Arg (Figure 3C). Similarly, the reduced fraction of Cys132 is increased to 25% in Ala26Pro, 45% in Trp59Arg, and 57% in Leu128Arg. Because both Cys51 and Cys132 become much more reduced, there is a large cellular fraction of the mutant proteins that do not have the Cys51-Cys132 disulfide bond, or the Cys43-Cys51 and Cys132-Cys135 disulfide bonds. Without these stabilizing disulfide bonds, a major fraction of the mutant proteins is destabilized from the closed conformation. The redox state change of Cys43 and Cys135, however, are less significant in these mutants than in wild-type VKOR. Cys16, Cys85, and Cys96 stay in a highly reduced state in the wild-type and WR mutants and they can be viewed as controls because they do not form disulfide bonds or participate in catalysis.

Another interesting feature is the redox states of 2 active site cysteines, Cys132 and Cys135, which exist in cells in an equilibrium of R, PO, and O states.<sup>32,42</sup> The peptides containing both

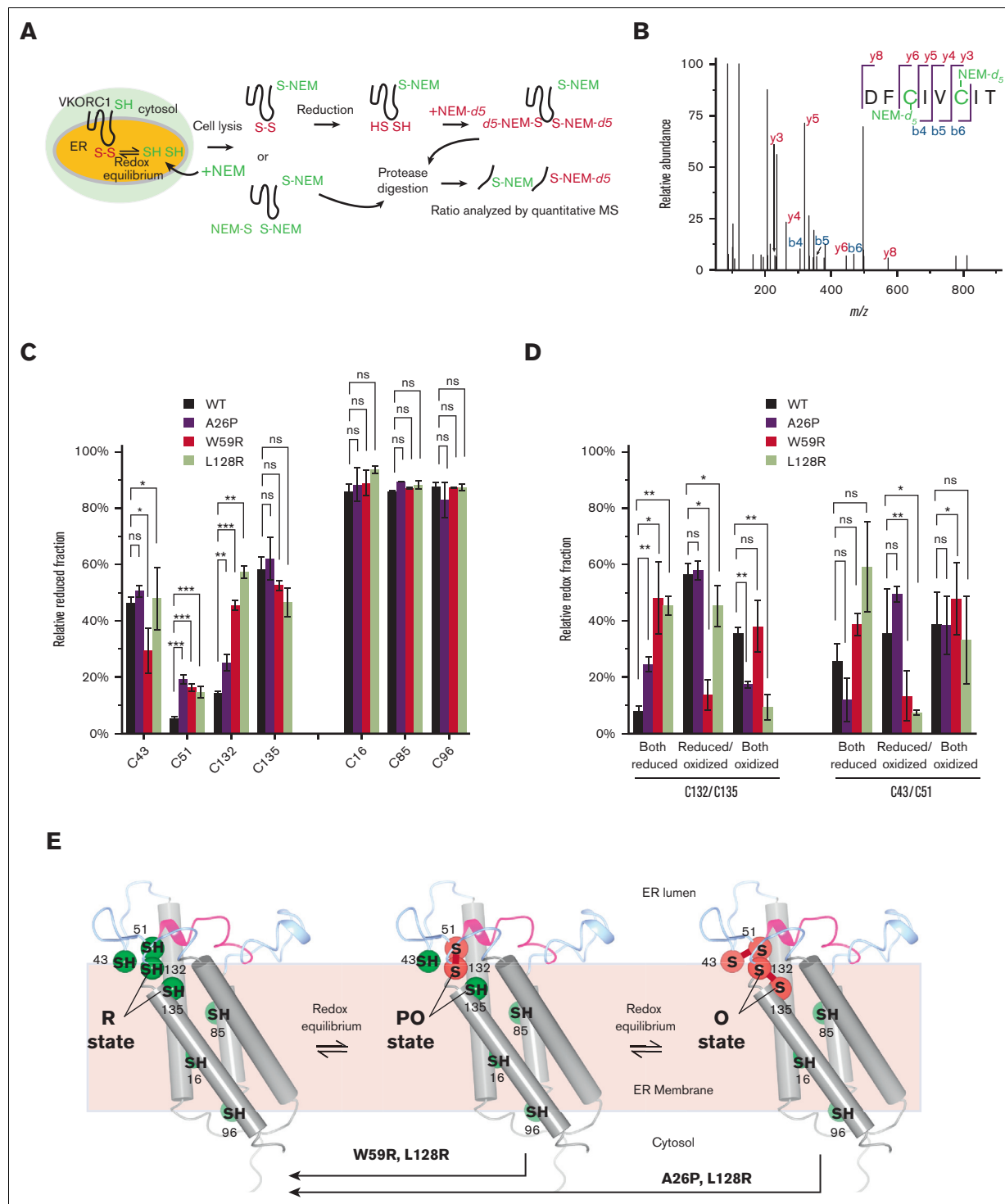


**Figure 3. MS-based footprinting reveals that severe WR mutants induce the shift of the VKOR active site to an aberrantly reduced state.** (A) Scheme of MS-based footprinting. VKOR cysteines located in the ER are in equilibrium between oxidized and reduced states, and those in the cytosol or inside the ER membrane remain reduced. The membrane permeable NEM (ie, NEM- $d_0$ ) is used to label all reduced cysteines in cells. After cell lysis, the oxidized cysteines are subsequently reduced by tris(2-carboxyethyl) phosphine hydrochloride (TCEP), labeled by the NEM- $d_5$  isotopologue, resulting in a mixture of  $d_0$  and  $d_5$  proteins, and digested. MS quantification to provide the ratio of the isotopically labeled peptides gives the redox state of each cysteine in the cells. (B) Representative product-ion (MS/MS) spectrum of a peptide with both Cys132 and Cys135 labeled by NEM- $d_5$ . (C) Relative reduced levels of cysteines in WT VKOR and severe WR mutants. All 3 severe WR mutants shift Cys51 and Cys132 to an aberrantly reduced state. As controls, Cys16 (TM1), Cys85 (TM2), and Cys96 (cytosolic loop) remain in the reduced state in WT and mutants. The error bars are from 3 different peptides and two-tailed student *t* test are used. \* $P < .05$ , \*\* $P < .01$ , \*\*\* $P < .001$ . (D) Relative redox fractions of cysteine pairs. The severe WR mutants shift Cys132/Cys135 at the active site to an aberrantly reduced state. (E) Structural interpretation of MS detected the state of VKOR cysteines. Severe WR mutants shift the cellular state of Cys132/Cys135 from PO or O state to R state. WT, wild-type.

Cys132 and Cys135 were analyzed by MS footprinting (Figure 3D). In wild-type VKOR, the R state (8%) is much less abundant than the PO (57%) and O states (36%) that are preferentially inhibited by warfarin.<sup>32,47</sup> Remarkably, MS footprinting of the severe WR mutants shows that the cellular abundance of the R state increases to 25%, 48%, and 45% in Ala26Pro, Trp59Arg, and Leu128Arg, respectively (Figure 3D), which is 3- to 6-fold higher than that of wild-type VKOR. Thus, the active site of these WR mutant proteins is substantially reduced in cells. With a large cellular fraction in the R state, warfarin binding is prohibited.<sup>32,47</sup>

## Severe WR mutations induce the exposure of active site to the aberrant reduction

To understand the cause of the increased level of R state in WR mutants, we performed MD simulation based on a highly accurate (2.0 Å) crystal structure of wild-type VKOR in the closed conformation.<sup>43</sup> For the 3 severe WR mutants, the starting models for MD are also reliable because only a single mutation (Ala26Pro, Trp59Arg, or Leu128Arg) is made on the wild-type crystal structure. Repeated assessments of MD simulation (100 ns each) showed that these mutations largely increase the flexibility of the regions forming the active site. Compared with wild type, Trp59Arg shows an increase of up to 1.3 Å RMSF in the region capping the active site (Figure 4A), whereas other parts of the Trp59Arg structure have RMSFs similar to those of wild-type VKOR. This is because Trp59 is a central residue of the capping region, and Trp59Arg changes this large aromatic residue to a charged residue and breaks the membrane association of part of the cap region. The RMSF of Ala26Pro increases by ~0.5 to 0.9 Å in the helical extension of transmembrane helix (TM1) and 1 to 1.6 Å in the domain anchoring the cap region but is similar to the RMSF of wild-type VKOR in other structural regions (Figure 4B). This Ala26Pro mutation breaks the helix formation and as a result, TM1 extension loses its interaction with the anchor domain. As to Leu128Arg, the cap helix loses its helical conformation, and a large movement is observed in the loop before this helix (Figure 4C). Although Leu128 is on a loop between TM3 and TM4, this loop forms stabilizing interactions with the cap helix. Thus, losing this interaction increases the flexibility of the cap region. Overall, owing to the increased flexibility of the cap region and TM1 extension, the active sites of these mutants become abnormally exposed to small reducing molecules in the ER, such as GSH (Figure 4D). The GSH reduction results in the large increase of the level of R state in these mutants, explaining the observations from MS footprinting (Figure 3C-D).

## Discussion

The phenotypes of WR mutants are associated with their redox state. Only with their redox state maintained as in cells, most WR mutants exhibit resistance *in vitro*, and their IC<sub>50</sub>s correspond well to the severities and dosage requirements during anticoagulation therapy. Severe WR is caused by the abnormal shift to R state in these mutants, resulting in high residual activity not inhibited by warfarin (Figure 5).

Activity from the increased R state further explains the general lack of VKCFD in patients and their family members carrying the WR mutations. This lack of a discernible defect in the physiological function of VKOR is consistent with the *in vitro* assays showing that WR mutants have activities similar to that of wild-type VKOR<sup>32,39,40</sup>

(Figure 1D). Such retained activities have been puzzling because WR mutations should interfere with both VKOR catalysis and warfarin inhibition, as substrates and warfarin are bound in the same pocket, forming the active site<sup>43</sup> (Figure 1B). This puzzle can now be well explained because the activity loss due to disrupted substrate (eg, warfarin) binding by WR mutations is compensated by the increased R state induced by the same mutations (Figure 5). Our previous analysis shows that, for wild-type VKOR, the R state has approximately eightfold higher specific activity than the PO state (O state is catalytically inactive) and contributes about half of the total cellular activity.<sup>42</sup> In the severe WR mutants, the abundance of the R state is drastically increased (3- to 6-fold), and, therefore, their activity should be increased accordingly over that of wild-type VKOR. These expected large increases in activity, however, are not observed (Figure 1D), implying that the mutations also impair substrate binding. Owing to these 2 counteracting effects (ie, impaired substrate binding and increased R state), WR mutants show comparable activity ranging from slightly lower to even higher than the wild-type VKOR (Figure 1D). Consequently, there are no adverse coagulation events due to VKCFD associated with the population carrying WR mutations.

The severe resistance phenotype of the WR mutations originates from mutually strengthening factors. First, these mutations artificially increase the R state level, generating a high warfarin-uninhibited activity that manifests as apparent WR. This residual activity is not inhibited by warfarin because the R state has low binding affinity for warfarin.<sup>32,42,47</sup> The poor inhibition of the R state is supported by observations from the DTT-driven assay, in which VKOR is nearly completely shifted to R state by this strong reductant (redox potential -330 mV). DTT reduction is detrimental to warfarin binding; with DTT, warfarin inhibition of the wild-type VKOR is weakened to a level similar to the strongest WR mutations (Figure 1C,E). Interestingly, wild-type VKOR in DTT shows large residual activity at high warfarin concentration (Figure 1C), similar to the behavior of severe WR mutants in GSH (Figure 2). This similarity indicates that both cases share the same underlying mechanism of abnormal shift to the R state. Because DTT shifts even wild-type VKOR to the R state, the relative resistance of most WR mutants becomes indiscernible in DTT. Although it has been known that WR phenotype cannot be reproduced in DTT,<sup>49</sup> the underlying mechanism was never truly understood. For instance, DTT reduction was postulated to interfere with warfarin inhibition via bypassing the electron-transfer process.<sup>49</sup> Here, the actual cause is identified: both the apparent resistance of wild-type VKOR in DTT and the phenotype of severe WR mutants are attributed to the abnormal shift to the R state.

Apart from R state shift, WR mutations weaken warfarin binding via disrupting warfarin interactions and/or destabilizing the cap domain.<sup>43,46</sup> Among the 9 strong WR mutants (displaying > 5-fold resistance), residues Val54, Trp59, Ile123, Leu128, and Tyr139 form part of the warfarin-binding pocket.<sup>43</sup> Val54Leu introduces a larger side chain that likely narrows the size of the warfarin-binding pocket. Trp59Arg, Ile123Asn, and Leu128Arg likely interfere with the nonpolar interactions of these residues with the aromatic ring of warfarin. Tyr139His mutation may alter the hydrogen bonding with the 4-hydroxyl group of warfarin.<sup>43</sup> On the other hand, Ala26, Val29, and Ala34 are in the helical extension of TM1, a structural region that stabilizes the cap domain via indirect interactions.<sup>43,46</sup> Consequently, the mutations on these residues may destabilize the cap domain.



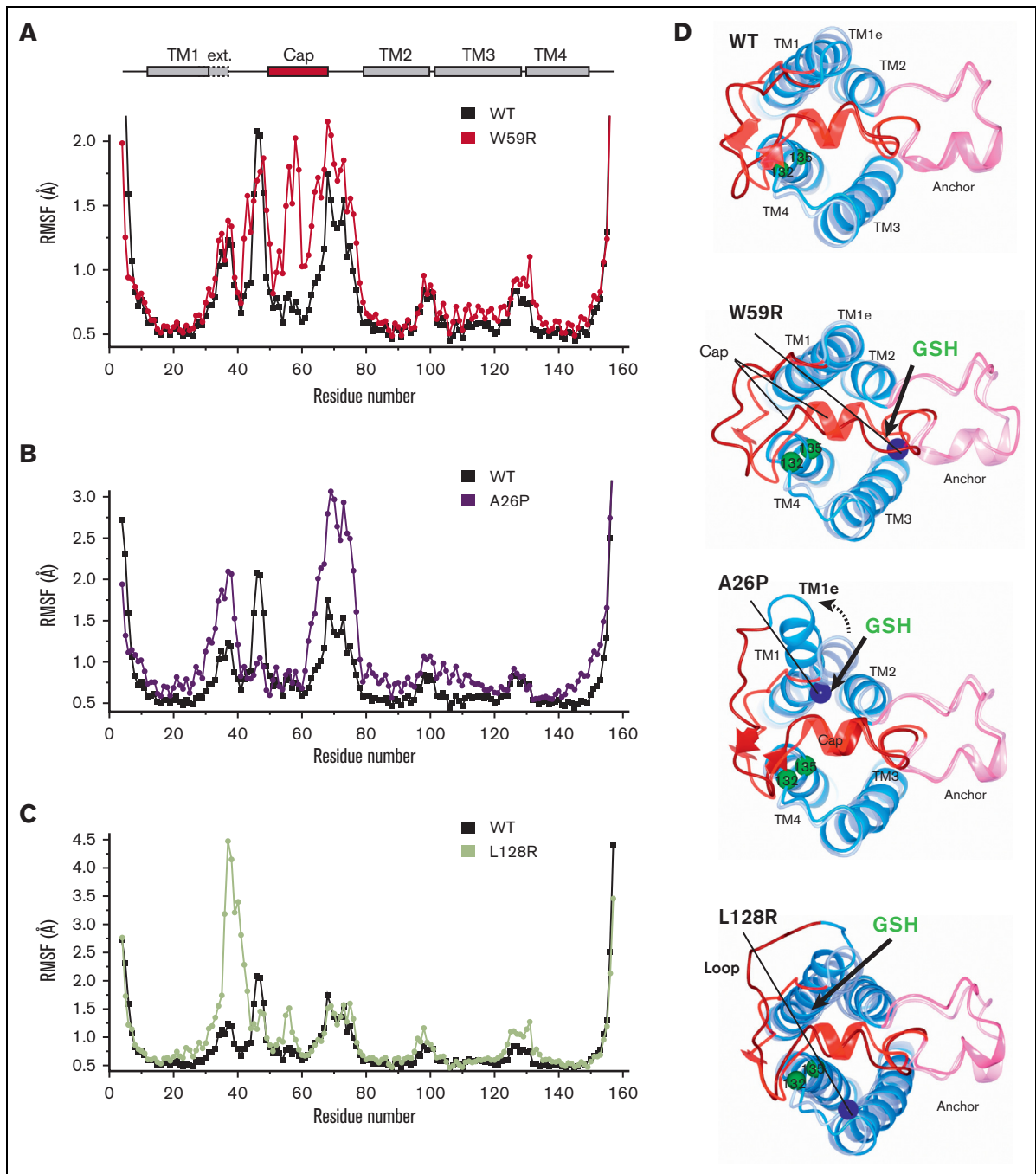


**Figure 4. MD simulation shows that severe WR mutations expose the VKOR active site for GSH reduction.** (A) RMSF comparison shows that Trp59Arg mutation induces large movement of the cap domain. (B) RMSF comparison shows that Ala26Pro induces aberrant movements in the TM1 helical extension and in the anchor domain. (C) RMSF comparison shows that Leu128Arg induces movements of a loop preceding the cap domain. All MD simulations (100 ns) were repeated 3 times and similar results were obtained. (D) The structural movements expose the active site for GSH reduction. Cys132 and Cys135 are shown in green spheres and Trp59Arg, Ala26Pro, and Leu128Arg in blue. For WT and each mutant, the starting MD model is shown in light blue, pink, and red colors, and a representative conformation during the MD simulation is shown in darker colors. Full structural movements during the 100 ns simulation are shown in supplemental Movie 1. The arrows indicate the opening of the sites to which GSH may gain access. TM1e, helical extension of TM1; WT, wild-type.

For different WR mutants, relative contributions from inducing R state shift and directly affecting warfarin binding can be deduced from the relative resistance levels with GSH (as in cells) or DTT (Figure 1E). With DTT reduction, both WR mutants and wild-type

VKOR are fully converted to the R state. With this factor eliminated, Val54Leu and Tyr139His retain similar resistance in DTT, GSH, and in cells. Thus, these mutations should directly affect warfarin binding, consistent with their structural interpretation<sup>43</sup>:

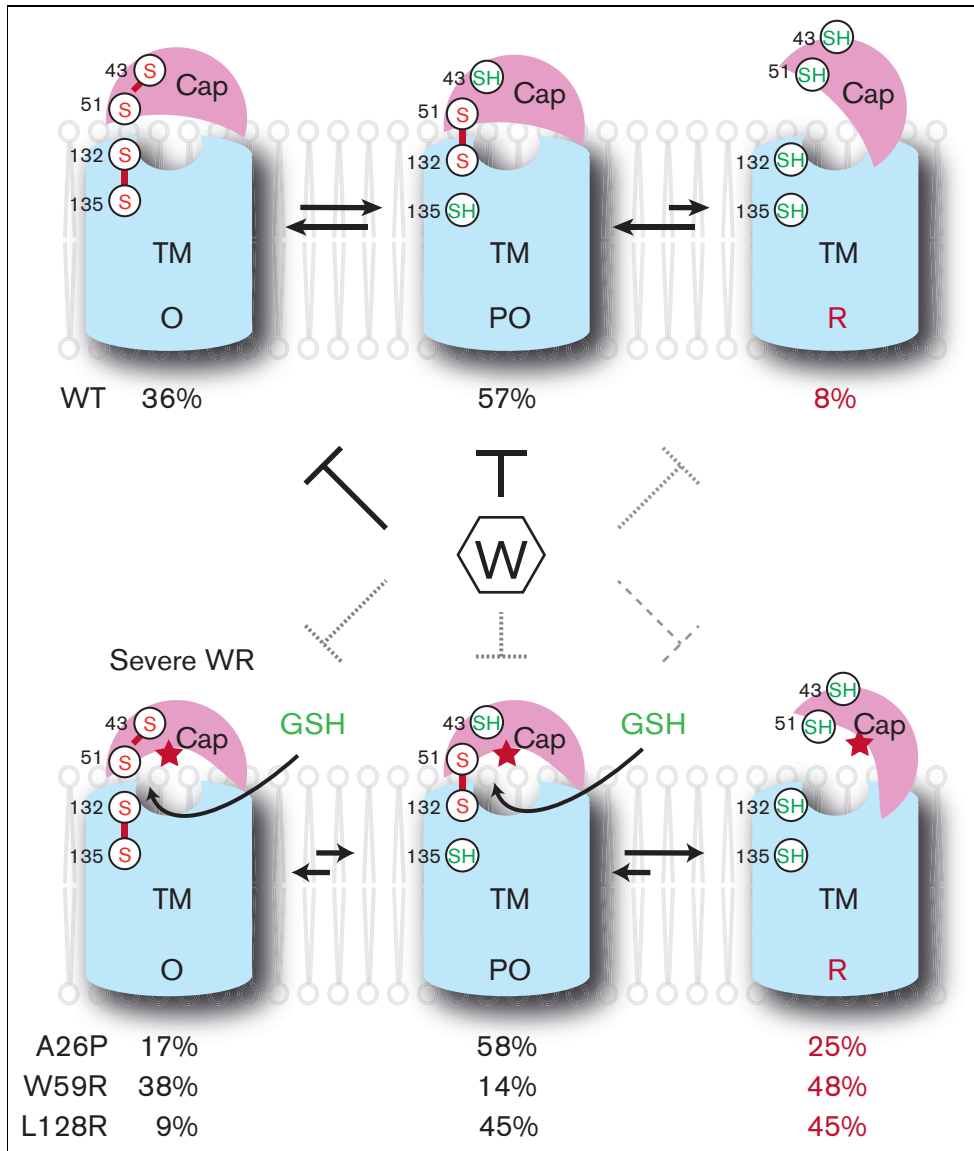


**Figure 5. Mechanism of severe WR mutations.** Top, in the cellular environment, wild-type (WT) VKOR is largely oxidized (O and PO state), and only a small fraction is in the R state. The fractions of these states are measured by in-cell MS footprinting (Figure 2A). The arrows indicate redox equilibrium, and the short arrow indicates a small propensity for shifting to the R state. Bottom, severe WR mutations (indicated by red star) hinder warfarin binding (dashed lines) and increase the exposure of the VKOR active site to GSH. The increased GSH reduction generates high levels of the R state that is poorly inhibited by warfarin (thin dashed line), resulting in large warfarin-uninhibited activity that manifests as severe WR. In absence of warfarin, the high R state activity compensates for weakened substrate binding, explaining the general lack of VKCFD phenotype.

Val54Leu alters the pocket size and Tyr139His is relatively deep in the membrane and not directly associated with the cap domain. Conversely, Ala26Pro, Trp59Arg, and Leu128Arg show large differences in their resistance to GSH and DTT, indicating a significant contribution from the R state shift. Remarkably, these 3 mutations also show the strongest resistance and the largest warfarin-uninhibited activity (Figures 1E and 2). Therefore, the most severe WR phenotype largely originates from the R state shift.

Owing to the R state shift, severe WR mutants are intrinsically uninhibited by warfarin. From our data, we have generated a reference table (Table 1) to guide distinction between mutants that are uninhibited by warfarin. Additionally, mutations on residues (eg, Asp44)

identified from alanine scanning mutagenesis can cause strong WR.<sup>32</sup> In practice, patients displaying signs of severe WR should be considered for alternative treatments with novel oral anticoagulants.

## Acknowledgments

W.L. is supported by National Heart, Lung, and Blood Institute (R01 HL121718), W. M. Keck Foundation (Forefront of Science Award), American Heart Association (20CSA35310354), Children's Discovery Institute (MCII 2020-854), and National Institute of Allergy and Infectious Diseases (R01 AI158500). The mass spectrometry measurement is supported by National Institute of General Medical Sciences (P41 GM103422 and R24

GM136766) to M.L.G. and National Institute of General Medical Sciences (R01 GM131008) to W.L. and M.L.G.

## Authorship

Contribution: S. Li performed the experiments with help from S. Liu; J.S. performed MS analysis; W.L. did the MD simulation with help from F.Z.; W.L. designed and oversaw the study and analyzed the results; W.L. and S.Li. wrote the manuscript; and M.L.G. edited the manuscript.

Conflict-of-interest disclosure: The authors declare no competing financial interests.

ORCID profiles: J.S., 0000-0001-8775-5032; F.Z., 0000-0002-6852-2994; W.L., 0000-0002-8711-1904.

Correspondence: Weikai Li, Department of Biochemistry and Molecular Biophysics, Washington University in St. Louis School of Medicine, 660 S. Euclid Ave, St. Louis, MO 63110; email: [weikai@wustl.edu](mailto:weikai@wustl.edu).

## References

1. Goy J, Crowther M. Approaches to diagnosing and managing anticoagulant-related bleeding. *Semin Thromb Hemost.* 2012;38(7):702-710.
2. Merli GJ, Fink J. Vitamin K and thrombosis. *Vitam Horm.* 2008;78:265-279.
3. Shea MK, Holden RM. Vitamin K status and vascular calcification: evidence from observational and clinical studies. *Adv Nutr.* 2012;3(2):158-165.
4. Schurgers LJ. Vitamin K: key vitamin in controlling vascular calcification in chronic kidney disease. *Kidney Int.* 2013;83(5):782-784.
5. Fouque D, Vennegoor M, Wee PT, et al. EBPG guideline on nutrition. *Nephrol Dial Transplant.* 2007;22(suppl 2):ii45-ii87.
6. Klack K, de Carvalho JF, El Asmar MS, Naoum JJ, Arbid EJ. Vitamin K dependent proteins and the role of vitamin K2 in the modulation of vascular calcification: a review. *Oman Med J.* 2014;46(3):398-406.
7. Bügel S. Vitamin K and bone health in adult humans. *Vitam Horm.* 2008;78:393-416.
8. Pearson DA. Bone health and osteoporosis: the role of vitamin K and potential antagonism by anticoagulants. *Nutr Clin Pract.* 2007;22(5):517-544.
9. Chu P-H, Huang T-Y, Williams J, Stafford DW. Purified vitamin K epoxide reductase alone is sufficient for conversion of vitamin K epoxide to vitamin K and vitamin K to vitamin KH<sub>2</sub>. *Proc Natl Acad Sci U S A.* 2006;103(51):19308-19313.
10. Stafford DW. The vitamin K cycle. *J Thromb Haemost.* 2005;3(8):1873-1878.
11. Oldenburg J, Marinova M, Müller-Reible C, Watzka M. The vitamin K cycle. *Vitam Horm.* 2008;78:35-62.
12. Wadelius M, Pirmohamed M. Pharmacogenetics of warfarin: current status and future challenges. *Pharmacogenomics J.* 2007;7(2):99-111.
13. Au N, Rettie AE. Pharmacogenomics of 4-hydroxycoumarin anticoagulants. *Drug Metab Rev Vol.* 2008;40(2):355-375.
14. Geisen C, Watzka M, Sittinger K, et al. VKORC1 haplotypes and their impact on the inter-individual and inter-ethnic variability of oral anticoagulation. *Thromb Haemost.* 2005;94(4):773-779.
15. Rieder MJ, Reiner AP, Gage BF, et al. Effect of VKORC1 haplotypes on transcriptional regulation and warfarin dose. *N Engl J Med.* 2005;352(22):2285-2293.
16. Wigle TJ, Jansen LE, Teft WA, Kim RB. Pharmacogenomics guided-personalization of warfarin and tamoxifen. *J Pers Med.* 2017;7(4):20.
17. Watzka M, Geisen C, Bevans CG, et al. Thirteen novel VKORC1 mutations associated with oral anticoagulant resistance: insights into improved patient diagnosis and treatment. *J Thromb Haemost.* 2011;9(1):109-118.
18. Harrington DJ, Gorska R, Wheeler R, et al. Pharmacodynamic resistance to warfarin is associated with nucleotide substitutions in VKORC1. *J Thromb Haemost.* 2008;6(10):1663-1670.
19. Bodin L, Perdu J, Diry M, Horellou MH, Lorient MA. Multiple genetic alterations in vitamin K epoxide reductase complex subunit 1 gene (VKORC1) can explain the high dose requirement during oral anticoagulation in humans. *J Thromb Haemost.* 2008;6(8):1436-1439.
20. Rost S, Fregin A, Ivaskevicius V, Conzelmann E, Hortnagel K. Mutations in VKORC1 cause warfarin resistance and multiple coagulation factor deficiency type 2. *Nature.* 2004;427(6974):537-541.
21. Pelz H-j, Rost S, Hünerberg M, et al. The genetic basis of resistance to anticoagulants in rodents. *Genetics.* 2005;170(4):1839-1847.
22. D'Ambrosio RL, D'Andrea G, Cafolla A, Faillace F, Margaglione M. A new vitamin K epoxide reductase complex subunit-1 (VKORC1) mutation in a patient with decreased stability of CYP2C9 enzyme. *J Thromb Haemost.* 2007;5(1):191-193.
23. Harrington DJ, Underwood S, Morse C, Shearer MJ, Tuddenham EG, Mumford AD. Pharmacodynamic resistance to warfarin associated with a Val66Met substitution in vitamin K epoxide reductase complex subunit 1. *Thromb Haemost.* 2005;93(1):23-26.
24. Loebstein R, Dvoskin I, Halkin H, et al. A coding VKORC1 Asp36Tyr polymorphism predisposes to warfarin resistance. *Blood.* 2007;109(6):2477-2480.
25. Hodroge A, Matagrín B, Moreau C, et al. VKORC1 mutations detected in patients resistant to vitamin K antagonists are not all associated with a resistant VKOR activity. *J Thromb Haemost.* 2012;10(12):2535-2543.
26. De Vilder EY, Debacker J, Vanakker OM. GGCC-associated phenotypes: an overview in search of genotype-phenotype correlations. *Int J Mol Sci.* 2017;18(2):240.
27. Czogalla KJ, Biswas A, Rost S, Watzka M, Oldenburg J. The Arg98Trp mutation in human VKORC1 causing VKCFD2 disrupts a di-arginine-based ER retention motif. *Blood.* 2014;124(8):1354-1362.

28. Spronk HM, Farah RA, Buchanan GR, Vermeer C, Soute BA. Novel mutation in the  $\gamma$ -glutamyl carboxylase gene resulting in congenital combined deficiency of all vitamin K-dependent blood coagulation factors. *Blood*. 2000;96(10):3650-3652.
29. Rost S, Fregin A, Koch D, Compes M, Müller CR, Oldenburg J. Compound heterozygous mutations in the  $\gamma$ -glutamyl carboxylase gene cause combined deficiency of all vitamin K-dependent blood coagulation factors. *Br J Haematol*. 2004;126(4):546-549.
30. International Warfarin Pharmacogenetics C, Klein TE, Altman RB, et al. Estimation of the warfarin dose with clinical and pharmacogenetic data. *N Engl J Med*. 2009;360(8):753-764.
31. Tie JK, Jin DY, Tie K, Stafford DW. Evaluation of warfarin resistance using transcription activator-like effector nucleases-mediated vitamin K epoxide reductase knockout HEK293 cells. *J Thromb Haemost*. 2013;11(8):1556-1564.
32. Shen G, Cui W, Zhang H, et al. Warfarin traps human vitamin K epoxide reductase in an intermediate state during electron transfer. *Nat Struct Mol Biol*. 2017;24(1):69-76.
33. Li S, Liu S, Liu XR, Zhang MM, Li W. Competitive tight-binding inhibition of VKORC1 underlies warfarin dosage variation and antidotal efficacy. *Blood Adv*. 2020;4(10):2202-2212.
34. Shen G, Li S, Cui W, et al. Membrane protein structure in live cells: methodology for studying drug interaction by mass spectrometry-based footprinting. *Biochemistry*. 2018;57(3):286-294.
35. Vanommeslaeghe K, Hatcher E, Acharya C, et al. CHARMM general force field: a force field for drug-like molecules compatible with the CHARMM all-atom additive biological force fields. *J Comput Chem*. 2010;31(4):671-690.
36. Van Der Spoel D, Lindahl E, Hess B, Groenhof G, Mark AE, Berendsen HJC. GROMACS: fast, flexible, and free. *J Comput Chem*. 2005;26(16):1701-1718.
37. Huang J, Rauscher S, Nawrocki G, et al. CHARMM36m: an improved force field for folded and intrinsically disordered proteins. *Nat Methods*. 2017;14(1):71-73.
38. Oldenburg J, Muller CR, Rost S, Watzka M, Bevans CG. Comparative genetics of warfarin resistance. *Hämostaseologie*. 2014;34(2):143-159.
39. Chen X, Jin DY, Stafford DW, Tie JK. Evaluation of oral anticoagulants with vitamin K epoxide reductase in its native milieu. *Blood*. 2018;132(18):1974-1984.
40. Czogalla KJ, Biswas A, Wendeln A-C, et al. Human VKORC1 mutations cause variable degrees of 4-hydroxycoumarin resistance and affect putative warfarin binding interfaces. *Blood*. 2013;122(15):2743-2750.
41. Li S, Liu S, Yang Y, Li W. Characterization of warfarin inhibition kinetics requires stabilization of intramembrane vitamin K epoxide reductases. *J Mol Biol*. 2020;432(18):5197-5208.
42. Shen G, Cui W, Cao Q, et al. The catalytic mechanism of vitamin K epoxide reduction in a cellular environment. *J Biol Chem*. 2021;296:100145.
43. Liu S, Li S, Shen G, Sukumar N, Krezel AM, Li W. Structural basis of antagonizing the vitamin K catalytic cycle for anticoagulation. *Science*. 2021;371(6524):eabc5667.
44. Hwang C, Sinsky AJ, Lodish HF. Oxidized redox state of glutathione in the endoplasmic reticulum. *Science*. 1992;257(5076):1496-1502.
45. Montero D, Tachibana C, Winther JR, Appenzeller-Herzog C. Intracellular glutathione pools are heterogeneously concentrated. *Redox Biol*. 2013;1(1):508-513.
46. Shen G, Li S, Cui W, et al. Stabilization of warfarin-binding pocket of VKORC1 and VKORL1 by a peripheral region determines their different sensitivity to warfarin inhibition. *J Thromb Haemost*. 2018;16(6):1164-1175.
47. Fasco MJ, Principe LM, Walsh WA, Friedman PA. Warfarin inhibition of vitamin K 2,3-epoxide reductase in rat liver microsomes. *Biochemistry*. 1983;22(24):5655-5660.
48. Krishna Kumar D, Gopal Shewade D, Parasuraman S, et al. Estimation of plasma levels of warfarin and 7-hydroxy warfarin by high performance liquid chromatography in patients receiving warfarin therapy. *J Young Pharm*. 2013;5(1):13-17.
49. Rishavy MA, Usualieva A, Hallgren KW, Berkner KL. Novel insight into the mechanism of the vitamin K oxidoreductase (VKOR): electron relay through Cys43 and Cys51 reduces VKOR to allow vitamin K reduction and facilitation of vitamin K-dependent protein carboxylation. *J Biol Chem*. 2011;286(9):7267-7278.